

Aluminium Two Thousand World Congress and International Conference on Extrusion and Benchmark ICEB 2015

Effect of microstructure and casting defects on the mechanical properties of secondary AlSi10MnMg(Fe) test parts manufactured by vacuum assisted high pressure die casting technology

A. Niklas^a, A. Bakedano^a, S. Orden^b, M. da Silva^{c,d}, E. Nogués^c, A.I. Fernández-Calvo^{a,*}

^aIK4-AZTERLAN, Engineering, R&D and Metallurgical Processes, Aliendalde Auzunea 6, Durango E-48200, Spain

^bTQC Technologies, Aliendalde Auzunea 10-1B, Durango E-48200, Spain

^cFundació Privada Ascamm, Parc Tecnològic del Vallès, Av. Universitat Autònoma 23, Cerdanyola del Vallès E-08290, Spain

^dUniversitat Autònoma de Barcelona, Plaça Cívica s/n, Campus de la UAB, Cerdanyola del Vallès E-08193, Spain

Abstract

Primary AlSi10MnMg alloy is widely used for manufacturing of high ductility VPDC castings. This alloy combines low Fe with high Mn level to guarantee good ductility. Secondary alloys are cheaper but they contain a higher Fe content, which is detrimental to the ductility. Microadditions based on Mn have been found very effective in formation of less harmful α -iron compounds.

In this study the effect of microstructure and casting defects on mechanical properties has been investigated in secondary alloy with 0.62%Fe and moderate Mn. Mechanical properties similar to the primary alloy were obtained when specimens were free from casting defects.

© 2015 Published by Elsevier Ltd.

Selection and Peer-review under responsibility of Conference Committee of Aluminium Two Thousand World Congress and International Conference on Extrusion and Benchmark ICEB 2015

Keywords: High Pressure Die Casting HPDC; Vacuum; Intermetallic Iron Compounds; Secondary Alloy; Ductility

* Corresponding author. Tel.: +0034-94 621 5470; fax: +0034 – 94 621 5471.

E-mail address: afernandez@azterlan.es

1. Introduction

Primary aluminium-silicon-magnesium alloys are by far the most widely used type in the manufacturing of safety parts for the automotive industry, such as suspension components and wheels, due to their excellent castability and good mechanical properties [1] which can be further improved by heat treatment: solution treatment followed by water quenching and subsequent artificial aging T6 or T7. Until the introduction of thin walled structural parts in the 1990's, these safety critical components were mostly produced in permanent mould. The more recent structural castings, being extremely thin walled (of the order of 2.5 mm) and of large dimensions usually require the use of high pressure die casting. These parts must be free of defects and heat treatable in order to attain the requested properties. Vacuum has to be applied for achieving ductility and weldability and precautions relative to the die design, die lubricant, melt quality and shot profile are also mandatory.

Conventional HPDC alloys are usually secondary alloy, in which iron is intentionally in the range of 0.8-1.1 wt. % in order to prevent molten metal soldering to the die [2-4]. However, conventional HPDC alloys and processes are not employed for high ductility castings and safety parts due to the presence of large β -Al₅FeSi compounds. For this reason, the primary AlSi10MnMg alloys with a maximum iron content of 0.25 wt. % and high Mn to avoid die soldering were developed [5]. Nevertheless, the use of recycled alloys with high iron content can reduce significantly the production costs of a part by increasing die life. It should be noted that die manufacturing and maintenance make up more than 10 % of HPDC manufacturing. Additionally, secondary alloys are cheaper and their production requires much less energy and generates less CO₂ emissions.

It is well known that addition of elements such as Mn, Cr, Sr, Co, Be and Ca can neutralize the effect of the brittle β iron compounds by substituting them by α -iron compounds with a less harmful morphology. The effect of these microadditions on the iron compounds in aluminium casting alloys has been investigated by several authors [6-11].

The present work investigates the microstructure and mechanical properties of both, a primary alloy with high Mn and low Fe content and a secondary AlSi10MnMg(Fe) alloy with high iron content and moderate addition of Mn in a step test part, manufactured by VPDC technology in the as cast and T6 heat treated condition. The effect of casting defects on mechanical properties, in particular ductility has also been studied.

2. Experimental procedure

A Buhler cold chamber HPDC machine with a maximum locking force of 5250 kN, a plunger with a diameter 60 mm and a stroke of 450 mm was used in the tests. In the first step of the injection process the plunger was constantly accelerated in order to reduce the gas entrapment during this phase. The velocity was kept constant in the second phase, filling of the die cavity. The plunger velocity was 4.5 m/s in order to ensure the filling of the section of 1 mm. The metal velocity at the ingate section was 44 m/s. A VDS vacuum system, activated and deactivated by interaction with HPDC machine, was used. A ProVac Ultra Easy 2000 valve and a ProVac CV 300 chill vent were employed to achieve a vacuum level between 85 and 100 mbars. The vacuum in the die allowed also the proper filling during the second phase. The third phase, the compression phase, started when the plunger felt a backpressure. The metal pressure was between 900 and 950 bars in the compression phase. For each experiment, 350 kg of each alloy were melted in an electric furnace. The alloys were modified using AlSr10 master alloy, pure Mg was added in order to keep the concentration of Mg between 0.3 wt. % and 0.40 wt. % in the melt. The melt was degassed with argon using a rotor impeller reaching D₈₀ values of more than 2.62 g/cm³. The control of oxides was also made using the K-Mould. An automatic ladle was used to extract the metal from the furnace at a temperature between 700 °C and 720 °C and pour into the shot sleeve.

The chemical compositions of the alloys used in this work are presented in Table 1. Alloy A is a typical primary AlSi10MnMg alloy for VPDC castings with a Mn content of 0.68 wt. % and low Fe content of 0.17 wt. %. Alloys B is a secondary alloy with 0.62 wt. % of Fe and a Mn content of 0.42 wt. %. The Mn content has been optimised previously [11] regarding the elimination of β -iron compounds. The higher Cu and Zn content present in alloy B in comparison to the primary variant, is typical of recycled aluminium. The primary alloy presents a slightly higher Mg content. Both alloys have Sr addition for eutectic Si modification. The total of Mn + Fe is higher in alloy B (1.04 wt. %) than in alloy A (0.85 wt. %), this is expected to have a positive effect with respect to die soldering.

According to the Gobrecht [12] at a pouring temperature around 680 °C (typical of HPDC process), the sludge factor, $SF = [\%Fe] + 2[\%Mn] + 3[\%Cr]$ should be less than 2.2. As it is shown in Table 1, both alloys present a similar value (alloy A: 1.53 and alloy B: 1.49 wt. %) and are well below 2.2. Thus, the precipitation of coarse intermetallics is not expected.

Table 1. Chemical composition (wt. %)

Alloy	Si	Fe	Cu	Mn	Mg	Cr	Ni	Zn	Ti	Sr	Total Fe+Mn	SF
A-Primary*	10.7	0.17	<0.01	0.68	0.47	<0.01	0.01	0.01	0.05	0.0061	0.85	1.53
B-Secondary	10.1	0.62	0.04	0.42	0.37	0.01	0.01	0.03	0.04	0.0101	1.04	1.49

*The primary alloy corresponds to the quality ENAC 43.500 according to the norm UNE-EN 1706:2011.

The die was designed to fabricate a step test piece with a width of 170 mm and wall thicknesses of 1, 2, 4, 6, 10 and 15 mm [11]. Mechanical properties have been determined in the 2 and 4 mm steps. The characteristics and chemical composition of the intermetallic iron compounds were examined using scanning electron microscopy (SEM) with an energy dispersive X-ray spectrometer (EDS). For the quantification of area fraction of intermetallic compounds, twenty images were obtained at a magnification of 2000X. The area fraction of each compound was estimated using a LAS V4.2 image analyzer.

Both alloys were subjected to a T6 heat treatment consisting of solution treatment at 490 °C for 3 h, water quenched and aged at 165 °C for 3 h. The heat treatment has been optimized previously regarding solution temperature and time in order to avoid blister formation. Subsequently flat tensile specimens were prepared maintaining the casting skin and tested according to UNE-EN ISO 6892-1:2010.

3. Results and Discussion

3.1. Microstructure

The microstructures formed in the 2 mm step of the as cast (F) test piece of both, primary and secondary alloy, are shown Figure 1. The microstructures of the as cast alloys, F Temper (Figures 1a -1b) present the following phases: primary aluminium, eutectic Al-Si, Mg_2Si and $\alpha-Al_{15}(FeMn)_3Si_2$ and $\pi-FeMg_3Si_6Al_8$ intermetallic iron compounds. After T6 heat treatment no large Mg_2Si phases are observed indicating the solution heat treatment was effective. Furthermore, the eutectic Si grows in size and becomes globular; the iron compounds are not affected by T6 heat treatment (Figures 1d -1e). Additionally, small gas pores appear in the microstructure (Figures 1c and 1f).

The intermetallic iron compounds were characterized in the scanning electron microscope (Figure 2). In the microstructure of both alloys two sizes of α compounds can be observed. The large α compounds have a size between 10–16 μm and are probably primary phases which have formed in the shot sleeve, while the formation of the small α particles occurred during solidification in the die. No large β iron compounds (>20 μm) have been detected in both alloys.

The compositions of α and π compounds are summarized in table 2. The α iron compounds of both alloys have Fe and Mn in the composition. As expected from the chemical composition of the alloys used for manufacture of the test parts the α compounds have a higher Mn content in the primary alloy and a higher Fe content in the secondary alloy. Small quantities of Mn are also detected in π iron compounds; again its amount is higher in the primary alloy.

Table 2: Chemical composition of α and π compounds in wt. % determined by EDS analysis.

Alloy	Compound	Mg	Al	Si	Fe	Mn
Primary A	α	-	65.3	10.8	3.90	20.0
	π	4.73	75.3	16.4	1.04	2.53
Secondary B	α	-	65.4	9.70	12.7	12.2
	π	4.20	78.2	13.5	3.30	0.80

Figure 3 shows the area fraction of all intermetallic iron compounds in the steps of 1, 2, 4, 6 and 10 mm for both alloys. It can be seen that the primary alloy A shows a lower area fraction of intermetallic α iron compounds than the secondary alloy B. Furthermore, a small decrease of area fraction with reduction of wall thickness is observed.

Several authors observed the same decrease of area fraction when cooling rate increased, and they attributed this to a delay in the growth mechanism of the intermetallic iron compounds [13-14].

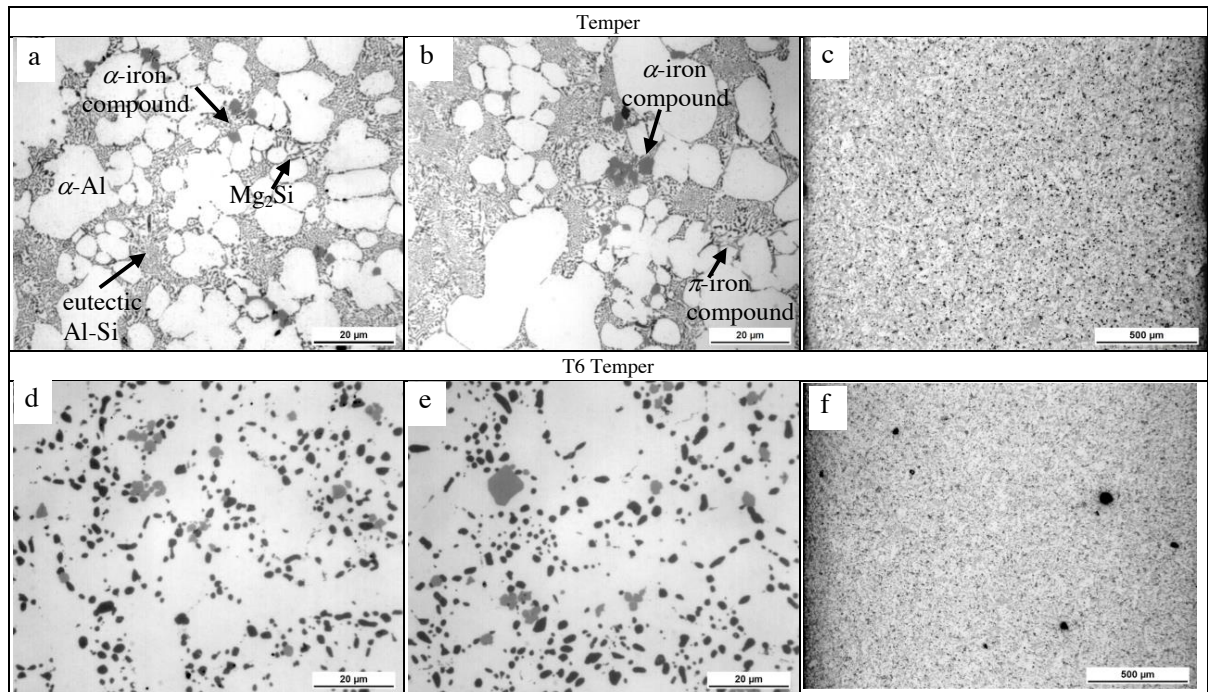


Figure 1. Microstructures observed in the 2 mm steps. Microstructures in the F temper: a) the primary alloy, b) and c) the secondary alloy; Microstructures in the T6 temper: d) the primary alloy, e) and f) the secondary alloy.

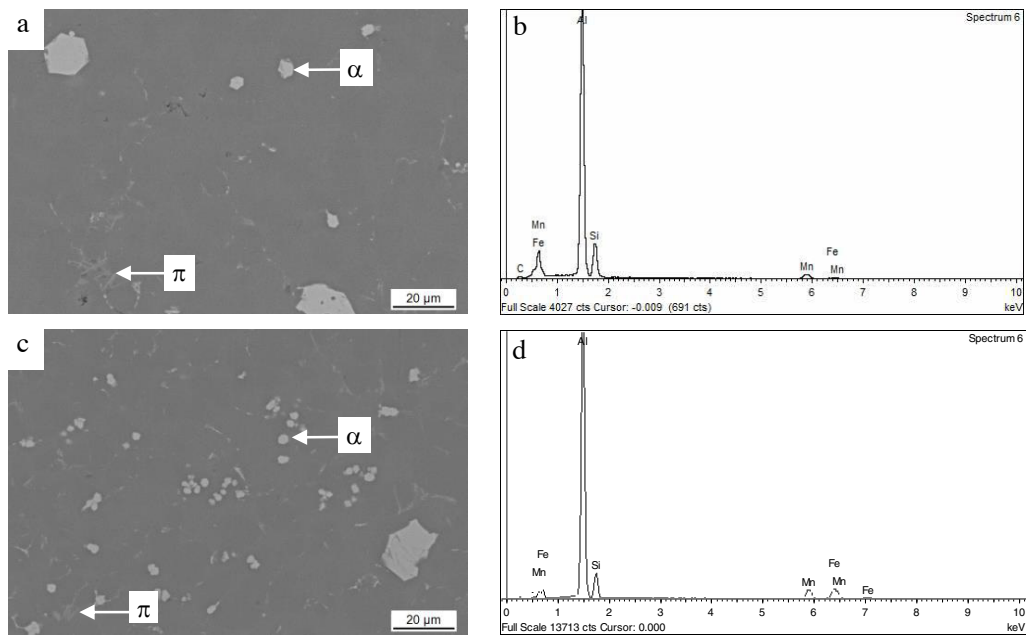


Figure 2. Intermetallic phases and EDS analysis of α phases in the 2 mm step, a) and b) the primary alloy; c) and d) the secondary alloy.

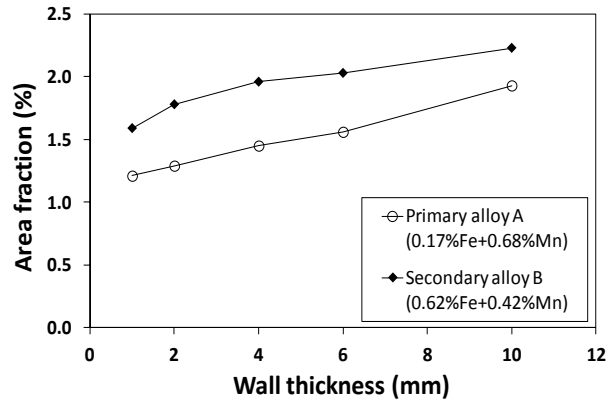


Figure 3. Effect of wall thickness on the area fraction of the intermetallic iron compounds.

3.2. Mechanical properties

The tensile properties of both alloys have been determined for the 2 mm step in F and T6 temper (see Table 3). The secondary alloy has been tested additionally in the 4 mm step. Macrographs of the corresponding fracture surfaces are shown in Table 4 and representative micrographs of the observed defects, lamination, cold shut, cold flake and gas porosity, are presented in Figure 5. Lamination and cold shuts occur if partially solidified layers of metal flows come together and do not knit. Whereas, cold flakes are formed when the molten metal is poured into the shot sleeve and a skin of solidified aluminium is pushed by the plunger into the die cavity during filling [15]. Gas porosity in HPDC is usually due to the decomposition of coolant and die lubrication or entrapped air [15, 16].

It can be observed, that elongation is strongly influenced by the presence of large sized casting defects, while the yield strength and ultimate tensile strength are less affected. The latter observation can be related to the orientation of defects with respect to the tensile direction. Aziz Ahamed et al. [18] reported that when the cold flakes are parallel or slightly inclined from the tensile direction no major effect on ultimate tensile strength is observed, while in case of perpendicular defects a linear decrease of tensile strength with the defect area occurred. In this study a reduction of elongation was observed as the size of the defect increases. Cold flakes/cold shuts/laminations, which have quite large sizes, reduce elongation significantly (Figure 6a). Whereas, the area fraction of gas porosity measured on the fracture surface of the test specimen was quite low (up to 0.35 % in the 2 mm step and 0.69 % in the 4 mm step) due to the application of vacuum in the die and hence elongation is less affected by these defects (Figure 6b). In both alloys high elongation values, above 7 %, are only obtained when the fracture surface is free from casting defects or its area fraction is low as in the case of gas porosity. The appearance of large sized defects was less frequent in the 2 mm step and thus also higher elongation was obtained.





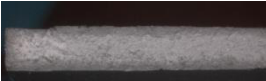


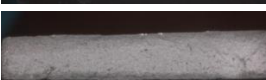
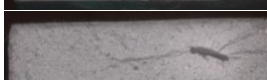
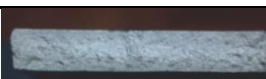


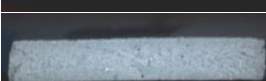
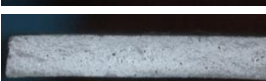

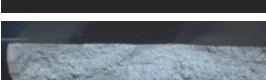
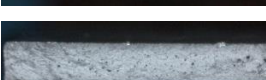

Table 3: Mechanical properties of the primary alloy A and secondary alloy B.

Sample		Primary alloy in the 2 mm step			Secondary alloy in the 2 mm step			Secondary alloy in the 4 mm step		
No.	Temper	Rp0.2 (MPa)	Rm (MPa)	E (%)	Rp0.2 (MPa)	Rm (MPa)	E (%)	Rp0.2 (MPa)	Rm (MPa)	E (%)
1	F	162	227	1.2	148	252	2.6	134	230	2.6
2		161	243	1.8	151	303	7.2	137	228	1.9
3		156	284	8.0	146	296	6.2	137	257	4.0
4	T6	272	326	7.3	223	284	7.5	217	284	6.1
5		275	329	6.9	214	275	5.7	230	277	2.3
6		275	325	6.5	227	291	8.3	243	258	0.5

In Figure 7 yield strength and elongation of both, primary and secondary alloy, are presented for the F and T6 temper. The mechanical property range of a commercial AlSi10MnMg primary alloy is also indicated. For the 2 mm

step it can be observed that both alloys are within the specified range of the primary alloy Trimal-05 [18]. However, the primary alloy A presents a higher yield strength and slightly lower ductility than the secondary alloy B in the T6-temper (Figure 7a). This could be at least in part due to the higher Mg content of the primary alloy A. In the F temper primary alloy presents slightly higher yield strength than the secondary alloy. For the 4 mm step most elongation values are below the specified values (Figure 7b), due to the presence of casting defects.

Table 4: Defects observed on the fracture surface of the tensile specimens of the primary alloy A and secondary alloy B.

Primary alloy in the 2 mm step				Secondary alloy in the 2 mm step		Secondary alloy in the 4 mm step	
Tem- No.	per	Defect	Fracture surface macrograph	Defect	Fracture surface macrograph	Defect	Fracture surface macrograph
1	F	Lamination		Cold flake		Cold flake	
2		Lamination		None		Cold shut	
3		None		Small oxide		Cold flake	
4	T6	None		Small gas pores		Small gas pores	
5		Small gas pores and small cold shut		Small gas pores		Cold flake and small gas pores	
6		Small gas pores		Small gas pores		Cold flake and gas pores	

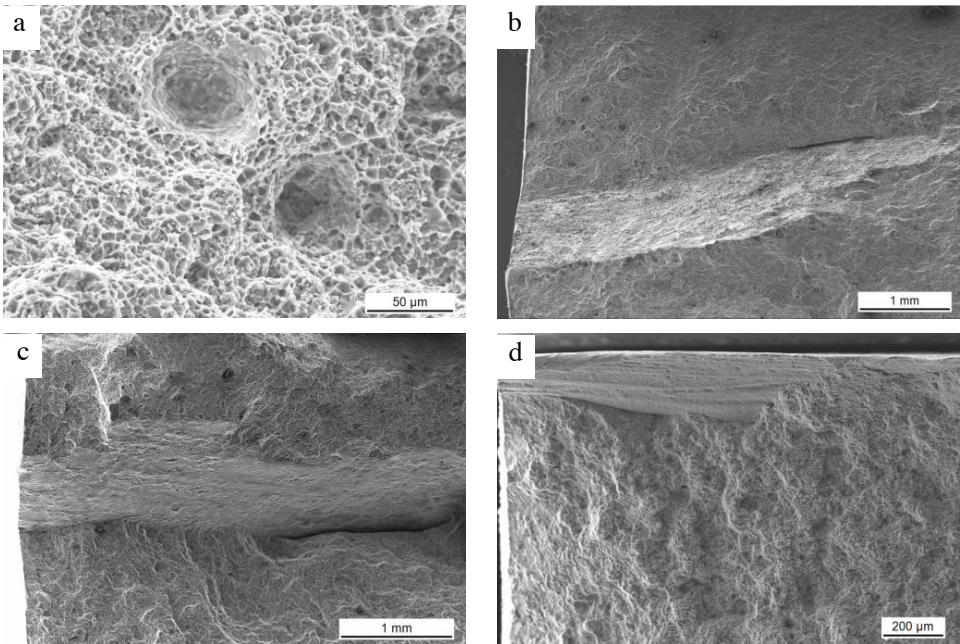


Figure 4. Observed casting defects: a) gas porosity, b) cold flake, c) cold shut and d) lamination.

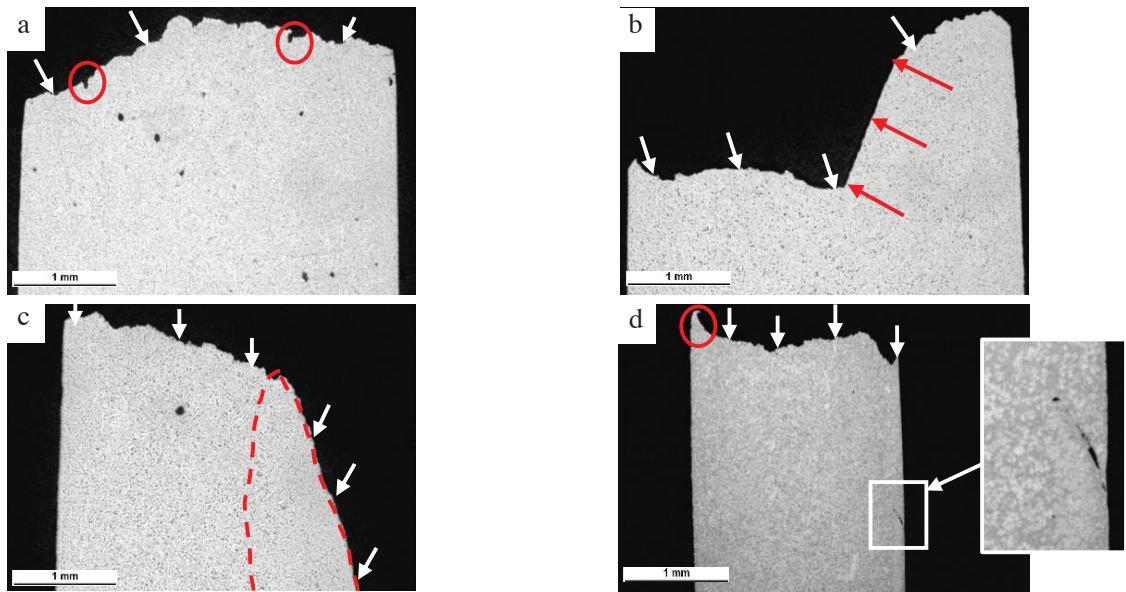


Figure 5. Metallographic section perpendicular to the fracture surface shown in Figure 4: a) gas porosity, b) cold flake, c) cold shut and d) lamination. Fracture surface is pointed by white arrows and defects on the fracture surface are indicated in dark colour.

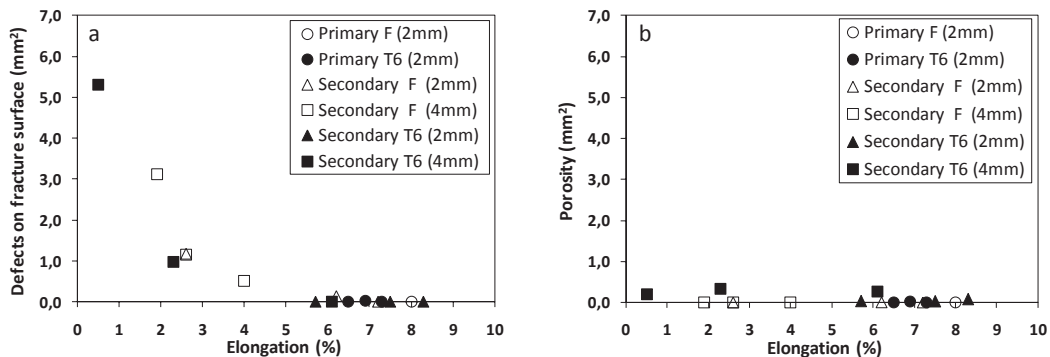


Figure 6. Effect of defect size on elongation of alloy A and B a) all defects except gas porosity and b) only gas porosity. Note: lamination defects are not measured because there are almost perpendicular to the fracture surface.

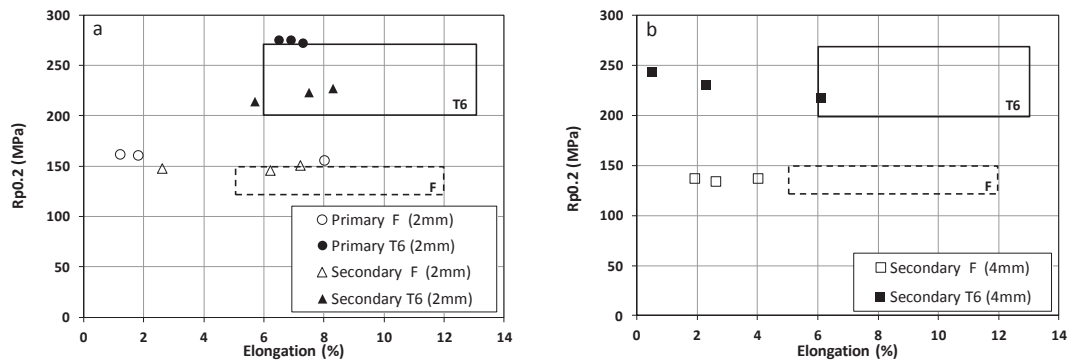


Figure 7. Mechanical properties of primary and secondary alloy in the F and T6 temper a) 2mm step and b) 4mm step. The mechanical property range of the primary AlSi10MnMg alloy Trimal-05 [18] in different tempers is indicated by rectangles.

4. Conclusions

In this work a secondary type AlSi10MnMg(Fe) alloy with 0.62 wt.% Fe and 0.42 wt. % Mn, has been cast in test parts with different wall thicknesses using VPDC technology. The effect of microstructure and casting defects on mechanical properties has been investigated in the F and T6 temper and compared to the corresponding AlSi10MnMg primary alloy. The following conclusions have been drawn:

- The addition of Mn was sufficient to avoid the presence of the needle/platelet shaped β -Al₅FeSi compounds, instead the polyhedral or Chinese script type α -Al₁₅(Fe,Mn)₃Si₂ is formed. The area fraction of the α iron compounds is higher in the secondary alloy.
- When the test specimens are free from casting defects or its area fraction is low, then mechanical properties similar to the corresponding primary alloy are achieved. The higher yield strength and ultimate tensile strength of the primary alloy has been attributed to its higher Mg content.
- The area fraction of gas porosity on the fracture surface was quite low (up to 0.35 % in the 2 mm step and 0.69 % in the 4 mm step) for both alloys. Hence, elongation was within the mechanical property range established for the AlSi10MnMg primary alloy produced by VPDC technology.
- The presence of casting defects such as laminations, cold shuts and cold flakes was found to reduce elongation significantly in both the primary and secondary alloy.

Acknowledgements

This research was financially supported by European Union's Seventh Framework Programme managed by REA – Research Executive Agency under grant agreement n° **315506** (FP7-SME-2012-1).

References

- [1] J. Gruzleski, B.M. Closset, The treatment of liquid aluminium-silicon alloys, American Foundry's Society, IL, 1990.
- [2] N.A. Belov, A.A. Aksenov, D.G. Eskin, Iron in aluminium alloys, Alloying Element, Taylor and Francis, New York, 2002.
- [3] D. Shankar Apelian, Materials Transaction, 2002, 33B pp. 465-476.
- [4] S.G. Shabestari, Materials Science Technology, 2004, A383-289.
- [5] H. Koch, U. Hielscher, H. Sternau, A. Franke, Silafont 36 high pressure die casting alloy, Light Metals, 1995, TMS pp. 1011-1018.
- [6] S. Murali, K.S. Raman, K.S.S. Murthy, Effect of trace additions (Be, Cr, Mn and Co) on the mechanical properties and fracture toughness of Fe- containing AlSi7Mg0.3 Alloy, Cast Met, 1994, vol. 6, pp.189-198.
- [7] S.S. Sreeja Kumari, R.M. Pillai, K. Nogita, A.K. Dahle, B.C. Pai, Influence of calcium on the microstructure and properties of an Al-7Si-0.3Mg-xFe alloy, Metallurgical and Materials Transactions A, 2006, vol. 37A, pp. 2581-2587.
- [8] G. Gustafsson, T. Thorvaldsson, G.L. Dunlop, The influence of Fe and Cr on the microstructure of cast Al-Si alloys, Metallurgical Transactions A, 1986, vol. 17A, pp. 45-52.
- [9] H.Y. Kim, S.W. Han, H.M. Lee, The influence of Mn and Cr on the tensile properties of A356–0.20Fe alloy, Materials Letter, 2006, vol. 60, pp. 1880-1883.
- [10] A.M. Samuel, F.H. Samuel, H.W. Doty, Observations on the formation of β -Al₅FeSi in 319 type Al-Si alloys, Journal of Material Science, 1996, vol. 31, pp. 5529-5539.
- [11] A. Bakedano, R. González-Martínez, A. Niklas, M. da Silva, M. Garat, A.I. Fernández-Calvo, Microstructural feature of primary and secondary ductile high pressure die casting alloys for the automotive industry, 71st World Foundry Congress, Bilbao, Spain, 19-21 May 2014.
- [12] J. Gobrecht, Schwerseigerungen von Eisen, Mangan und Chrom in Aluminium-Silicium-Gusslegierungen, Part 1: Giesserei 62, 1975, No.10 - Part 2: Giesserei 63, 1976, No. 20.
- [13] J. Espinoza-Cuadra, P. Gallegos-Acevedo, H. Mancha-Molinar Picado, Effect of Sr and solidification conditions on characteristics of intermetallic in Al-Si 319 industrial alloys, Materials and Design 3, 2010, pp. 343-356.
- [14] A. Verma, S. Kumar, P.S. Grant, K.A.Q. O'Reilly, Influence of cooling rate on the Fe intermetallic formation in an AA6063 Al alloy, Journal of Alloys and Compounds 555, 2013, pp. 274-282.
- [15] W.G. Walkington, Die casting defects – Causes and solutions, North American Die Casting Association, 2003.
- [16] G. Timelli, A. Fabrizi, The effects of microstructure heterogeneities and casting defects on the mechanical properties of high-pressure die-cast AlSi9Cu3(Fe) alloys, Metallurgical and Materials Trans. A, 2014, vol. 45A, pp. 5486-5498.
- [17] A.K.M. Aziz Ahamed, H. Kato, Influence of casting defects on tensile properties of ADC12 Aluminium alloy die-castings, Materials Trans., 2008, vol. 49, No.7, pp. 1621-1628.
- [18] Trimal®-05 data sheet, TRIMET Aluminium AG, Germany, www.trimet.de, 2008.